INTERACTION OF BRIGHT AND DARK SOLITARY WAVES IN A MULTICOMPONENT PLASMA WITH SUPERTHERMAL ELECTRONS FOR DIFFERENT COORDINATES SYSTEMS

M. Shokry
Department of Physics, Faculty of Science, Damietta University, New Damietta 34517, Egypt

Key Words: Planar/nonplanar of bright and dark ion acoustic solitary waves, The extended Poincaré-Lighthill-Kuo method, positive and negative ion fluids.

ABSTRACT

The interaction behavior of planar/nonplanar of bright and dark ion acoustic solitary waves (IASWs) in a multicomponent plasma composed of positive and negative ion fluids and kappa distributed superthermal electrons is investigated. For the generic case, the extended Poincaré - Lighthill - Kuo (PLK) method is employed to derive planar and nonplanar Korteweg-de Vries (KdV) equations and phase shift equations. The nonlinear propagation and the collision of planar/nonplanar bright and dark IASWs are studied. On the other hand, at a critical value of ion concentration, the extended PLK method is applied to obtain the modified planar/nonplanar KdV equations and their corresponding phase shifts. It is found that planar/nonplanar bright − planar/nonplanar dark IASWs can propagate and collide with each other. In all cases, the effects of several parameters such as: ion concentration, the position of IASWs, negative ion-to-positive ion mass ratio, the superthermality of electrons on the trajectories of planar/nonplanar bright and dark IASWs after collision are investigated. Numerical calculations lead to some highlights on the properties of IASWs (e.g., in laboratory plasmas such as laser–matter/plasma interaction experiments).

1. INTRODUCTION

The nonlinear planar/nonplanar ion acoustic solitary waves (IASWs), as one important nonlinear phenomena in a plasma, have been studied by many authors in various models of plasma physics in recent years [1-4]. Observation of ion acoustic solitons experimentally for first time [5], and in the years that followed, several studies of ion acoustic solitary waves have been discussed [6-8]. Furthermore, IASWs in multicomponent plasma have been studied by a number of authors resulting in a considerable success in clarifying many aspects of the characteristics of solitary planar [9, 10] and nonplanar systems [11-14]. An unmagnetized plasma consisting of warm adiabatic ions, superthermal electrons, and thermal positrons were considered [15]. This study may introduce a focus on the properties of ion acoustic solitary

waves in space and laboratory plasmas. Several theoretical and experimental investigations reports the importance of study of suprathermality in non-Maxwellian plasma particles which arise due to the influence of external fields acting on the space or laboratory plasmas (represented by a Kappa distribution) [16-20]. For example, the head-on collision of two concentric cylindrical ion acoustic solitary waves is discussed [21]. They showed new effects, geometric and dynamics which are absent in Cartesian solitons and could be tested in experimental nonlinear ion acoustic waves in plasma. Also, the head-on collision between two ion-acoustic solitary waves in an unmagnetized electron-positron-ion plasma has been investigated [22]. The effects of the ratio of electron temperature to positron temperature, and the ratio of the number density of positrons to that of electrons on the phase shift are studied. It is found that these parameters can significantly influence the phase shifts of the solitons and the compressive solitary wave can propagate in this system. Head-on collision of ion acoustic solitary waves in a three-component unmagnetized plasma with cold ions, Boltzmann distributed positrons, and superthermal electrons [23]. The effects of several plasma parameters such as: the ratio of electron temperature to positron temperature, the spectral index of the electron kappa distribution, and fractional concentration of positron component on the phase shift are studied. It is found that the superthermal electrons play a significant role on the collision of ion acoustic solitary waves. Continually; the nonlinear propagation of small but finite amplitude ion acoustic wave with superthermal electrons and positrons in a bi-ion collisionless plasma are discussed [24]. They have examined the effect of the electron superthermality on the ion acoustis soliton characteristics and insure supporting of their model to compressive as well as rarefactive solitary structures. An investigation to the head-on collision of cylindrical/spherical ion-acoustic solitary waves in an unmagnetized non-planar plasma consisting of warm adiabatic ions and nonthermally distributed electrons [25]. They found that the phase shifts induced by the collision of compressive and rarefactive solitary waves are very different. They also pointed out to the importance of these investigations about the observations of electrostatic solitary structures in astrophysical as well as in experimental plasmas with nonthermal energetic electrons.

The extended Poincaré - Lighthill - Kuo (PLK) method have been used to study the propagation and interaction between two solitary waves [26-32]. Great number of others studies the general case of solitary waves interaction by deriving the Korteweg-de Vries (KdV) equations and the corresponding phase shifts, and didn't mention the critical case of interaction. The one dimensional planar geometry and solitons interaction by deducing the modified KdV (mKdV) equations and their

corresponding phase shifts at the critical case [33-35]. Tile this moment, there is no detailed study for the difference between planar and nonplanar IASWs interaction in general and critical case. Thus, the purpose of this article is to study and compare the effect of different plasma parameters; negative ion-to-positive ion mass ratio, superthermal electron parameter on the behavior of planar and nonplanar ion acoustic solitary waves (IASWs) interactions in plasma. We organized this paper as follows. Sec. II includes the basic equations for planar and nonplanar IASWs including positive and negative ions and superthemal electrons. For generic case, the PLK method is introduced and the planar and nonplanar Korteweg–de Vries (KdV) equations are derived in order to describe the propagation of ion acoustic solitons, and in Sec. III we continue their corresponding phase shift. Furthermore, a modified planar and nonplanar Korteweg–de Vries (mKdV) equations with their corresponding phase shifts during interaction have been discussed at a critical case, Sec. IV. Numerical results and discussion are given in Sec. V.

II. THE GOVERNING EQUATIONS

We consider two fluids composed of positive and negative ions distinguished by using the index "+" and "-", and superthermal electrons. The planar and nonplanar dynamics of IASWs in multicomponent plasma are governed by [36]

$$\frac{\partial n_\pm}{\partial t} + \frac{\nu}{r}(n_\pm u_\pm) + \frac{\partial}{\partial r}(n_\pm u_\pm) = 0, \tag{1}$$

$$\frac{\partial u_\pm}{\partial t} + u_\pm \frac{\partial u_\pm}{\partial t} = \beta_\pm \frac{\partial \varphi}{\partial r}, \tag{2}$$

$$\frac{\nu}{r}\frac{\partial \varphi}{\partial r} + \frac{\partial^2 \varphi}{\partial r^2} = \mu_1 n_e + \mu_2 n_- - n_+, \tag{3}$$

where $\nu=0$ for planar geometry factor and $\nu=1$ and 2 for cylindrical and spherical (i.e., nonplanar) geometries factors, respectively. The variable $n_+(n_-)$ is the density of positive (negative) ions, $u_+(u_-)$ is the velocity of positive (negative) ions, φ, r, and t is the electrostatic potential, the space coordinate and time variables, respectively. In Eqs. 1-3, the ion density $n_+(n_-)$ is normalized by the unperturbed ion density $n_+^o(n_-^o)$, while u_+ (u_-) is normalized by the ion sound speed $c_s = \sqrt{(K_B T_e)/m_+}$. The variables n_e and φ are respectively normalized by the unperturbed electron density n_e^o and the thermal potential $(K_B T_e/eZ_+)$. The space coordinate is normalized by the Debye radius $\lambda_{D+}\left(= (K_B T_e/4\pi e^2 Z_+^2 n_{+0})^{\frac{1}{2}}\right)$ and the time is scaled by the ion plasma period $\omega_{p+}^{-1}(= (4\pi e^2 Z_+^2 n_{+0}/m_+)^{\frac{-1}{2}})$, where K_B is the Boltzmann constant and T_e is the

electron temperature. Here, $m_+ (m_-)$ is the positive (negative) ion mass and the positive ions charge $Z_+=1$. The dispersion relation implies $\mu_1 + \mu_2 = 1$, where $\mu_1 (= n_{e0}/n_{+0})$ and $\mu_2 (= n_{-0}/n_{+0})$.

The electrons number density n_e are assumed to possess superthermal distribution [36, 37]

$$n_e = \left(1 - \frac{\varphi}{\chi}\right)^{-\kappa + \frac{1}{2}},\tag{4}$$

which only valid for $\kappa > 3/2$, where κ is the superthermal parameter and $\chi = (\kappa - \frac{3}{2})$. The fluid equations are coupled through the Poisson's equation. We apply the extended PLK method to study planar and nonplanar IASWs interaction, so that, the following stretching is introduced [19, 29]

$$\xi = \varepsilon(r - \lambda t - r_1) + \varepsilon^2 P_o(\xi, \eta, R) + \dots,$$
$$\eta = \varepsilon(r + \lambda t - r_2) + \varepsilon^2 Q_o(\xi, \eta, R) + \dots,\tag{5}$$
$$R = \varepsilon^3 r.$$

The quantities $n_\pm, u_\pm$ and φ can be expanded about their equilibrium values in power series of ε as follows [21, 38]

$$n_\pm = 1 + \varepsilon n_\pm^{(1)} + \varepsilon^2 n_\pm^{(2)} + \varepsilon^3 n_\pm^{(3)} + \cdots,$$

$$u_\pm = \varepsilon u_\pm^{(1)} + \varepsilon^2 u_\pm^{(2)} + \varepsilon^3 u_\pm^{(3)} + \cdots,\tag{6}$$
$$\varphi = \varepsilon \varphi_1 + \varepsilon^2 \varphi_2 + \varepsilon^3 \varphi_3 + \cdots.$$

We introduce the following operators:

$$\hat{R} = \left(\frac{\partial}{\partial \xi} + \frac{\partial}{\partial \eta}\right), \qquad \widehat{R} = \left\{\frac{\partial}{\partial R} + \left(P_{0\xi} + P_{0\eta}\right)\frac{\partial}{\partial \xi}\right.$$
$$\left. + \left(Q_{0\xi} + Q_{0\eta}\right)\frac{\partial}{\partial \eta}\right\},$$

$$\hat{T} = \left(\frac{\partial}{\partial \eta} - \frac{\partial}{\partial \xi}\right), \qquad \widehat{T} = \lambda\left[\left(P_{0\eta} - P_{0\xi}\right)\frac{\partial}{\partial \xi} + \left(Q_{0\eta} - Q_{0\xi}\right)\frac{\partial}{\partial \eta}\right],$$

One can write these operators in a compact way, viz.

$$\frac{\partial}{\partial r} = \varepsilon \hat{R} + \varepsilon^3 \widehat{R} + \cdots, \qquad \frac{\partial}{\partial t} = \varepsilon \lambda \hat{T} + \varepsilon^3 \widehat{T} + \cdots,$$

To lowest nonzero order Eqs. 1–5 give

$$\lambda \hat{T} n_+^{(1)} + \hat{R} u_+^{(1)} = 0, \tag{7a}$$
$$\lambda \hat{T} n_-^{(1)} + \hat{R} u_-^{(1)} = 0, \tag{7b}$$
$$\lambda \hat{T} u_+^{(1)} + \hat{R} \varphi_1 = 0, \tag{7c}$$

$$\lambda \hat{T} u_-^{(1)} - \beta \hat{R} \varphi_1 = 0, \tag{7d}$$

$$\mu_1 \frac{\kappa - \frac{1}{2}}{\chi} \varphi_1 + \mu_2 n_-^{(1)} = \tag{7e}$$

$$n_+^{(1)}.$$

The solutions of Eqs. 7 can be given as

$$\varphi_1 = (\varphi_{1\xi} + \varphi_{1\eta}), \quad (8a)$$

$$n_+^{(1)} = \frac{1}{\lambda^2}(\varphi_{1\xi} + \varphi_{1\eta}), \quad (8b)$$

$$n_-^{(1)} = \frac{-\beta}{\lambda^2}(\varphi_{1\xi} + \varphi_{1\eta}), \quad (8c)$$

$$u_+^{(1)} = \frac{1}{\lambda}(\varphi_{1\xi} - \varphi_{1\eta}), \quad (8d)$$

$$u_-^{(1)} = \frac{-\beta}{\lambda}(\varphi_{1\xi} - \varphi_{1\eta}), \quad (8e)$$

$$\lambda = \sqrt{\chi(\mu_2\beta + 1)/\mu_1(\kappa - 1/2)}. \quad (8f)$$

After some algebraic manipulation we the next order in ε as

$$\lambda\hat{T}n_+^{(2)} + \hat{R}u_+^{(2)} + \hat{R}n_+^{(1)}u_+^{(1)} = 0, \quad (9a)$$

$$\lambda\hat{T}n_-^{(2)} + \hat{R}u_-^{(2)} + \hat{R}n_-^{(1)}u_-^{(1)} = 0, \quad (9b)$$

$$\lambda\hat{T}u_+^{(2)} + \hat{R}\varphi_2 + u_+^{(1)}\hat{R}u_+^{(1)} = 0, \quad (9c)$$

$$\lambda\hat{T}u_-^{(2)} - \beta\hat{R}\varphi_2 + u_-^{(1)}\hat{R}u_-^{(1)} = 0, \quad (9d)$$

$$\mu_1\frac{\kappa-\frac{1}{2}}{\chi}\varphi_2 + \mu_2 n_-^{(2)} + \mu_1\frac{\left(\kappa-\frac{1}{2}\right)\left(\kappa+\frac{1}{2}\right)}{2\chi^2}\varphi_1^2 - n_+^{(2)} = 0. \quad (9e)$$

By solving this system of Eqs we have

$$\varphi_2 = (\varphi_{2\xi} + \varphi_{2\eta} + \hat{\varphi}_2), \quad (10a)$$

$$n_+^{(2)} = \frac{1}{\lambda^2}(\varphi_{2\xi} + \varphi_{2\eta}) + \frac{3}{2\lambda^4}(\varphi_{1\xi}^2 + \varphi_{1\eta}^2) + \hat{n}_+, \quad (10b)$$

$$n_-^{(2)} = \frac{-\beta}{\lambda^2}(\varphi_{2\xi} + \varphi_{2\eta}) + \frac{3\beta^2}{2\lambda^4}(\varphi_{1\xi}^2 + \varphi_{1\eta}^2) + \hat{n}_-, \quad (10c)$$

$$u_+^{(2)} = \frac{1}{\lambda}(\varphi_{2\xi} - \varphi_{2\eta}) + \frac{1}{2\lambda^3}(\varphi_{1\xi}^2 - \varphi_{1\eta}^2) + \hat{u}_+, \quad (10d)$$

$$u_-^{(2)} = \frac{-\beta}{\lambda}(\varphi_{2\xi} - \varphi_{2\eta}) + \frac{\beta^2}{2\lambda^3}(\varphi_{1\xi}^2 - \varphi_{1\eta}^2) + \hat{u}_-. \quad (10e)$$

Here $\hat{\varphi}_2 = \varphi_2 - \varphi_{2\xi} - \varphi_{2\eta}$ has been defined as the part of φ_2 which depends on ξ, η and τ in a way which cannot be separated with similar definitions for other variables and higher orders [34].

The expressions in Eqs. 10 are coupled through

$$\delta_1\varphi_{1\xi}^2 = 0, \quad (11a) \qquad \delta_1\varphi_{1\eta}^2 = 0, \quad (11b)$$

and

$$\frac{\partial^2 \hat{\varphi}_2}{\partial \xi \partial \eta} + \delta_2 \frac{\partial \varphi_{1\xi}}{\partial \xi} \frac{\partial \varphi_{1\eta}}{\partial \eta} - \delta_2 \left(\varphi_{1\xi} \frac{\partial^2 \varphi_{1\eta}}{\partial \eta^2} + \varphi_{1\eta} \frac{\partial^2 \varphi_{1\xi}}{\partial \xi^2} \right) = 0, \qquad (11c)$$

where $\delta_1 = \left(\frac{\mu_1 \left(\kappa - \frac{1}{2} \right) \left(\kappa + \frac{1}{2} \right)}{\chi^2} - \frac{3(1 - \mu_2 \beta^2)}{\lambda^4} \right)$, and $\delta_2 = \frac{(1 - \mu_2 \beta^2)}{\lambda^2 (1 + \mu_2 \beta)}$.

It is clear that from Eq. 11, there exist two possibilities; one is called generic case, at $\varphi_{1\xi}^2 = \varphi_{1\eta}^2 = 0$, the other one is called critical case, at $\delta_1 = 0$.

III.GENERIC CASE:

The generic case can be achieved at $\varphi_{1\xi} = \varphi_{1\eta} = 0$ and thus find that the series expansion 5 go in even orders of ε much as is the case for the usual derivation of the KdV equation.

Finally, we arrive at the order to a set of equations where interesting new contributions appear:

$$\lambda \hat{T} n_+^{(4)} + \hat{T} n_+^{(2)} + \frac{\nu}{R} u_+^{(2)} + \hat{R} u_+^{(4)} + \hat{R} u_+^{(2)} + \hat{R} n_+^{(2)} u_+^{(2)} = 0, \qquad (12a)$$

$$\lambda \hat{T} n_-^{(4)} + \hat{T} n_-^{(2)} + \frac{\nu}{R} u_-^{(2)} + \hat{R} u_-^{(4)} + \hat{R} u_-^{(2)} + \hat{R} n_-^{(2)} u_-^{(2)} = 0, \qquad (12b)$$

$$\lambda \hat{T} u_+^{(4)} + \hat{T} u_+^{(2)} + u_+^{(2)} \hat{R} u_+^{(2)} + \hat{R} \varphi_4 + \hat{R} \varphi_2 = 0, \qquad (12c)$$

$$\lambda \hat{T} u_-^{(4)} + \hat{T} u_-^{(2)} + u_-^{(2)} \hat{R} u_-^{(2)} - \beta \hat{R} \varphi_4 - \beta \hat{R} \varphi_2 = 0, \qquad (12d)$$

$$\hat{Z} \varphi_2 - \mu_1 \frac{\kappa - \frac{1}{2}}{\chi} \varphi_4 - \mu_2 n_-^{(4)} + n_+^{(4)} - \mu_1 \frac{\left(\kappa - \frac{1}{2} \right) \left(\kappa + \frac{1}{2} \right)}{2 \chi^2} \varphi_2^2 = 0. \qquad (12e)$$

Now, combining the parts of Eq. 12 by using Eq. 10 which contain terms that only depend on ξ or on η(besides τ), yields the typical cylindrical Korteweg-de Vries (cKdV) equations

$$\frac{\partial \varphi_{2\xi}}{\partial R} + A \varphi_{2\xi} \frac{\partial \varphi_{2\xi}}{\partial \xi} + B \frac{\partial^3 \varphi_{2\xi}}{\partial \xi^3} + \frac{\nu}{2R} \varphi_{2\xi} = 0, \qquad (13)$$

$$\frac{\partial \varphi_{2\eta}}{\partial R} + A \varphi_{2\eta} \frac{\partial \varphi_{2\eta}}{\partial \eta} + B \frac{\partial^3 \varphi_{2\eta}}{\partial \eta^3} + \frac{\nu}{2R} \varphi_{2\eta} = 0. \qquad (14)$$

for the right- and left-going solitary waves, respectively, with the coefficient of the quadratic nonlinearity, A, and the dispersion coefficient B are given by $-B\delta_1$, and $\frac{\lambda^2}{2(\mu_2 \beta + 1)}$, respectively.

Furthermore, there is more information still, in the terms which contain both ξ and η, besides τ, giving

$$\frac{\partial^2}{\partial\xi\partial\eta}\left[\widehat{\varphi}_4 - S_1\varphi_{2\xi}\varphi_{2\eta}\right] + \frac{\partial}{\partial\xi}\left[\left(\frac{\partial P_0}{\partial\eta} + S\varphi_{2\eta}\right)\frac{\partial\varphi_{2\xi}}{\partial\xi}\right]$$
$$+ \frac{\partial}{\partial\eta}\left[\left(\frac{\partial Q_0}{\partial\xi} + S\varphi_{2\xi}\right)\frac{\partial\varphi_{2\eta}}{\partial\eta}\right] = 0, \tag{15}$$

with

$$S = \frac{B}{2}\left[\frac{(\mu_2\beta^2 - 1)}{\lambda^4} - \mu_1\frac{\left(\kappa - \frac{1}{2}\right)\left(\kappa + \frac{1}{2}\right)}{\chi^2}\right], \tag{16a}$$

$$S_1 = B\left[\frac{(1 - \mu_2\beta^2)}{\lambda^4} - \mu_1\frac{\left(\kappa - \frac{1}{2}\right)\left(\kappa + \frac{1}{2}\right)}{\chi^2}\right]. \tag{16b}$$

The second and third terms in Eq. 15 will generate secular contributions at the next higher order therefore we have:

$$\frac{\partial P_0}{\partial\eta} = S\varphi_{2\eta}, \qquad (17a \qquad \frac{\partial Q_0}{\partial\xi} = S\varphi_{2\xi}, \qquad (17b$$

In addition, the other remaining term in 15 will give rise to a contribution

$$\widehat{\varphi}_4 = S_1\varphi_{2\xi}\varphi_{2\eta}, \tag{18}$$

to φ_4, $\varphi_{2\xi}$ and $\varphi_{2\eta}$ parts, which will have to be determined from higher-order contributions.

For large R, the asymptotic solitary wave solutions of Eqs. 12 and Eqs.13 these are the well-known "sech squared" solitons of KdV theory, here [39-41]

$$\varphi_{2\xi} = \varphi_\xi\theta_1^{2\nu/3}\mathrm{sech}^2\left(\left(\frac{A\varphi_\xi}{12B}\right)^{1/2}\theta_1^{\nu/3}\left(\xi - \frac{1}{3}A\varphi_\xi\theta_1^{2\nu/3}R\right)\right), \tag{19}$$

$$\varphi_{2\eta} = \varphi_\eta\theta_2^{2\nu/3}\mathrm{sech}^2\left(\left(\frac{A\varphi_\eta}{12B}\right)^{1/2}\theta_2^{\nu/3}\left(\eta - \frac{1}{3}A\varphi_\eta\theta_2^{2\nu/3}R\right)\right), \tag{20}$$

where φ_ξ and φ_η are the amplitudes of solitons S_1 and S_2 in their initial positions. Here, the value of θ_1 and θ_2 are given by R_1/R, R_2/R, respectively, where $R_1 = \varepsilon^3 r_1$ and $R_2 = \varepsilon^3 r_2$. Now, the phase shift functions $P_0(\xi, \eta, R)$, and $Q_0(\xi, \eta, R)$ are obtained by substituting for $\varphi_{2\xi}$ and $\varphi_{2\eta}$ into Eq. 17, we have

$$P_0 = S\left(\frac{12B\varphi_\eta}{A}\right)^{1/2}\theta_2^{\nu/3}\left\{\tanh\left[\left(\frac{A\varphi_\eta}{12B}\right)^{1/2}\theta_2^{\nu/3}\left(\eta - \frac{1}{3}A\varphi_\eta\theta_2^{2\nu/3}R\right)\right] + 1\right\}, \tag{21}$$

$$Q_0 = S \left(\frac{12B\varphi_\xi}{A}\right)^{1/2} \theta_1^{\nu/3} \left\{\tanh\left[\left(\frac{A\varphi_\xi}{12B}\right)^{1/2} \theta_1^{\nu/3}\left(\xi - \frac{1}{3}A\varphi_\xi\theta_1^{2\nu/3}R\right)\right] - 1\right\}, \qquad (22)$$

where $\xi_{t=0} = \varepsilon(r_2 - r_1)$, $\eta_{t=0} = \varepsilon(r_1 - r_2)$, $\xi_t = \varepsilon[(r_2 - r_1) - 2\lambda t]$ and $\eta_t = \varepsilon[(r_1 - r_2) + 2\lambda t]$. So that, the trajectories of the two IASWs are given by

$$\xi = \varepsilon(r - \lambda t - r_1) - \varepsilon^2 S\left(\frac{12B\varphi_\eta}{A}\right)^{1/2} \theta_2^{\nu/3}$$
$$\left\{\tanh\left[\left(\frac{A\varphi_\eta}{12B}\right)^{1/2} \theta_2^{\nu/3}\left(\eta - \frac{1}{3}A\varphi_\eta\theta_2^{2\nu/3}R\right)\right] + 1\right\}, \qquad (23)$$

$$\eta = \varepsilon(r + \lambda t - r_2) - \varepsilon^2 S\left(\frac{12B\varphi_\xi}{A}\right)^{1/2} \theta_1^{\nu/3}$$
$$\left\{\tanh\left[\left(\frac{A\varphi_\xi}{12B}\right)^{1/2} \theta_1^{\nu/3}\left(\xi - \frac{1}{3}A\varphi_\xi\theta_1^{2\nu/3}R\right)\right] - 1\right\}, \qquad (24)$$

Using Eqs. 23 and Eqs. 24, the corresponding phase shifts are given by

$$\Delta P = 2\varepsilon^2 S\left(\frac{12B\varphi_\eta}{A}\right)^{1/2} \theta_2^{\nu/3}, \qquad (25)$$

$$\Delta Q = -2\varepsilon^2 S\left(\frac{12B\varphi_\xi}{A}\right)^{1/2} \theta_1^{\nu/3}, \qquad (26)$$
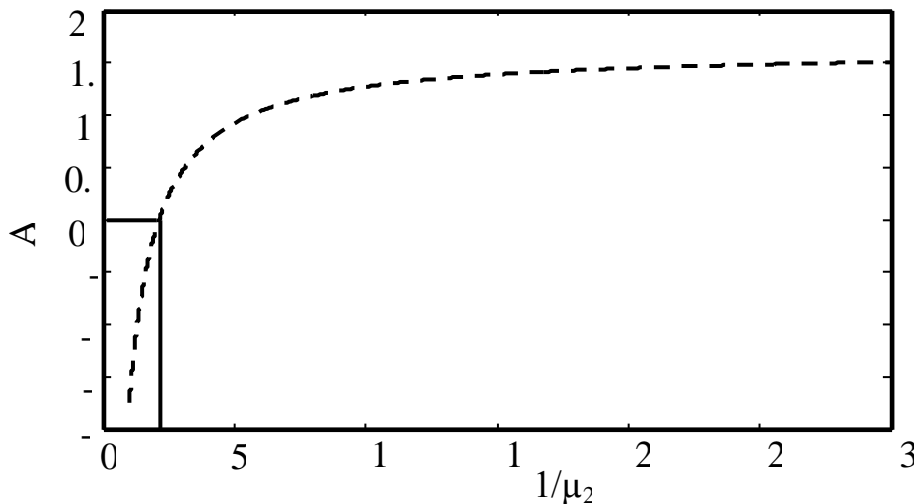

Fig. 1, The variation of nonlinear coefficient A, against $1/\mu_2$ for $\kappa = 1.8$, for planar and nonplanar geometry at $\varphi_{2\xi}=0.9$ $\varphi_{2\eta}=0.3$, $\varepsilon=0.1$, $\varphi_\eta =$

In this part of the present manuscript, we employed the extended PLK method to drive the planar and nonplanar Korteweg-de Vries (KdV) equations and phase shift equations are derived to investigate the future of IASWs after collision. Actually, it is valuable here mentioning that there exist two interacting solitons must have the same polarity given by the sign of AB. If AB > 0, both solitons must have positive polarity, but when AB < 0, both solitons must have negative polarity. Figure1 represents the relation between the amplitude of IASWs and the negative ion-to-positive ion density ratio μ_2. The ranges for the soliton polarities shown in Fig.1 agree with those found in recent head-on collisions of electrostatic solitons [33, 34]. Moreover, we consider two soliton S_1 is traveling to the right and soliton S_2 is traveling to the left, we see from Eqs. 25 and Eqs. 26 that due to collision, each soliton has a positive phase shift in its traveling direction. Physically, the positive phase shift means that IASWs increase their velocities during the collision stage [42].
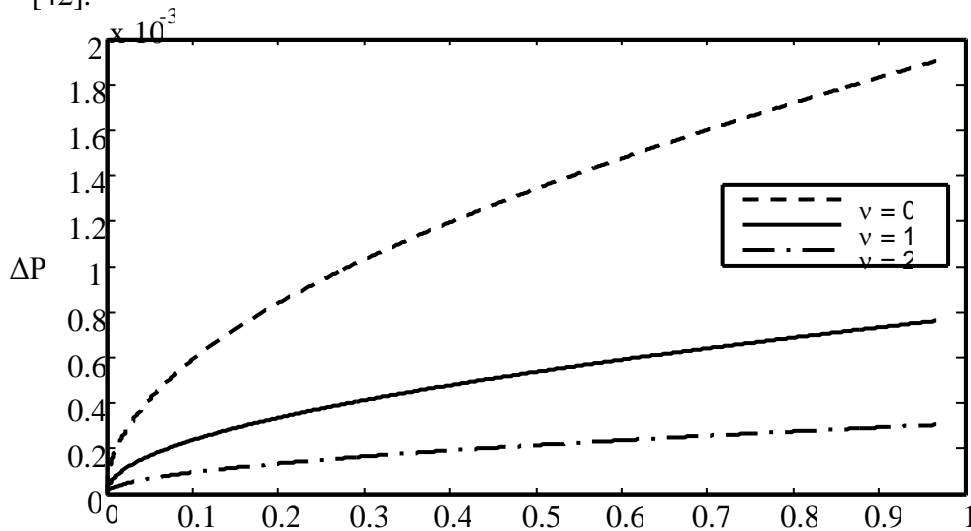

FIG. 2, The variation of the phase shift ΔP with μ_1 for planar geometry ($\nu = 0$), cylindrical geometry ($\nu = 1$) and for spherical geometry ($\nu = 2$) at $\varphi_{2\xi}$=0.9 $\varphi_{2\eta}$=0.3, ε=0.1, φ_η=0.1, φ_ξ=0.4

Figure 2 explores the differences in the phase shifts ΔP for planar and nonplanar (cylindrical/spherical) geometries. It is observed that the phase shifts ΔP is high for the planar geometry, intermediate for cylindrical geometry, while it is low for the spherical geometry. If we increase μ_1 to very large values the nonplanar geometries would approach the planar geometry. Therefore, the nature and the collision of

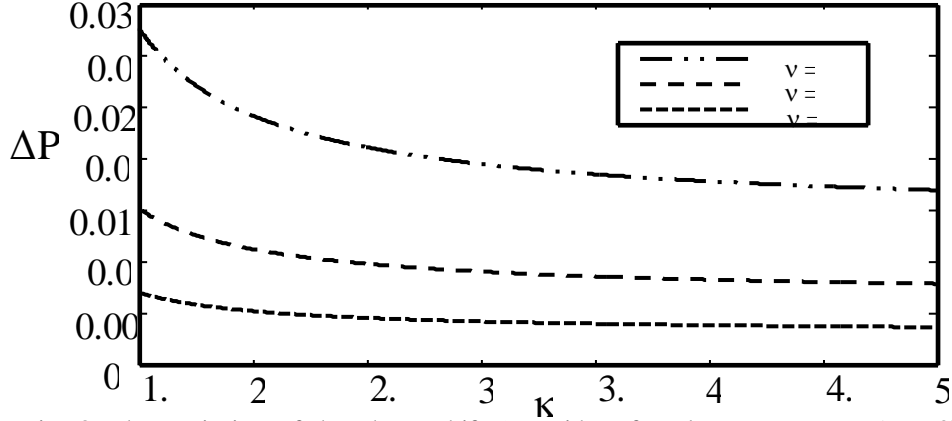IASWs significantly change for large values of μ_1, the scope of the present work.

Fig. 3, The variation of the phase shift ΔP with κ for planar geometry ($\nu = 0$), cylindrical geometry ($\nu = 1$) and for spherical geometry ($\nu = 2$) at $\varphi_{2\xi}$=0.9 $\varphi_{2\eta}$=0.3, ε=0.1, φ_{η}=0.1, φ_{ξ}=0.4

      Figure 3 presents the variation of the phase shift ΔP against the superthermal parameter κ for at the different values of $\nu = 0$, 1 and 2. For agiven ν, the phase shift ΔP decreases rabidly with κ when $\kappa \leq 2.5$ and increases smoothly with κ when $\kappa \geq 2.5$. For a given value of κ, the magnitude of the phase shift ΔP for the planar geometry is more than its value for the nonplanar geometry.
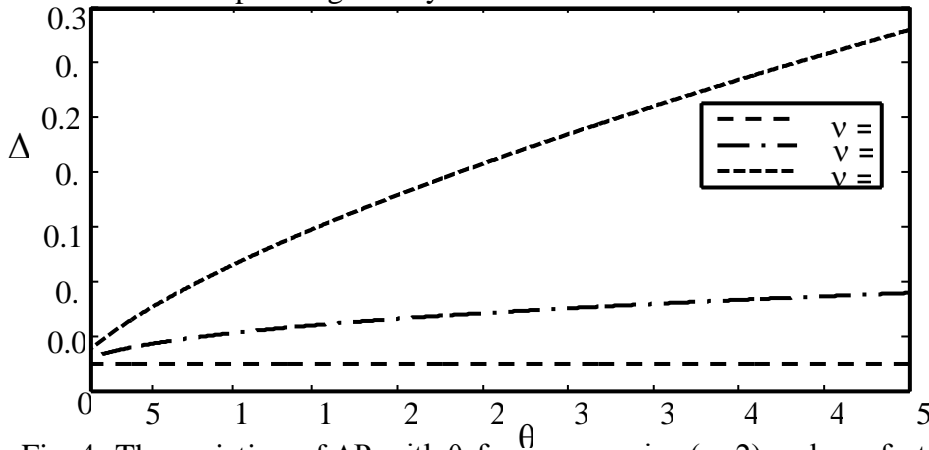

Fig. 4, The variation of ΔP with θ for compressive (μ=2) and rarefactive (μ=10) were ($\nu = 0$) for planar geometry, ($\nu = 1$) for cylindrical geometry, and ($(\nu = 2$) for spherical geometry

In Fig. 4 we have plotted the phase shifts variation against θ_1 for planar and nonplanar geometry. It is observed that: for a given value of ν, the phase shift ΔP increases with θ_1. For a given value of θ_1, the phase shift curves of the cylindrical geometry and the spherical geometry are fairly close to each other, whereas the phase shift curve for the planar geometry are comparatively far away from them.
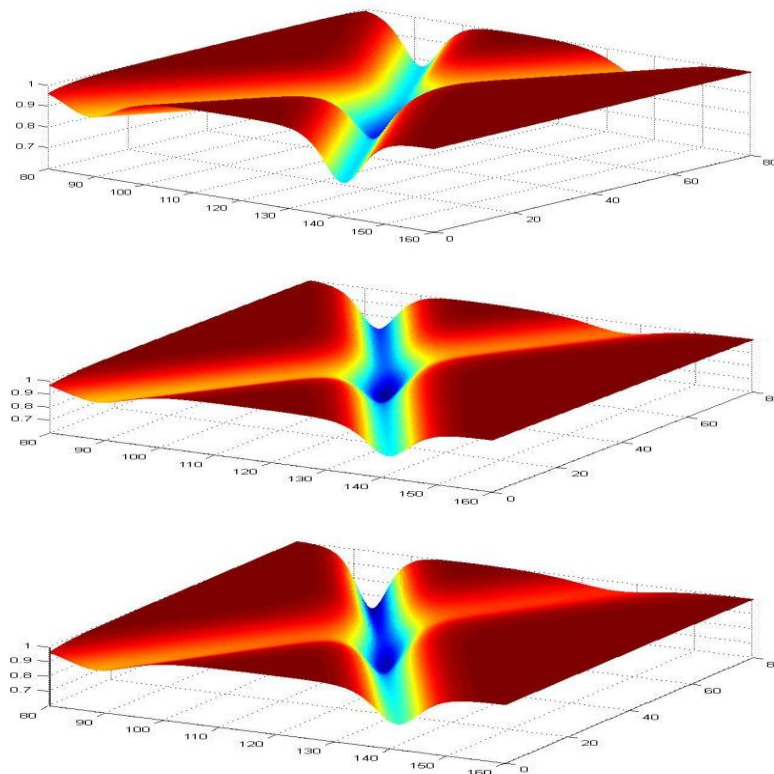

FIG. 5 the colliding process of two planar and nonplanar IASWs of rarefactive colliding process geometry at the same values as in fig.2

For planar, cylindrical and spherical geometries, Figs. 5 and 6 show the variation of the negative ion-to-positive ion density ratio against the space coordinate x and the time variable t, respectively. Additionally, Figures 5 and 6 demonstrate that two rarefactive and compressive IASWs propagate in opposite directions approach to each other, collide, and asymptotically separate away, respectively. We observe that during collision one practically motionless composite structure forms for some time interval.
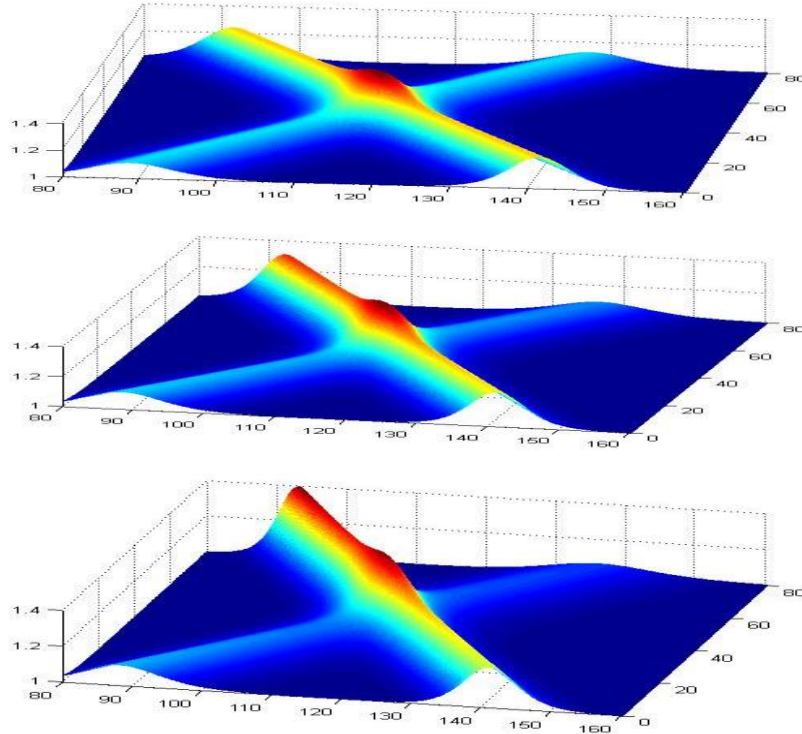
Fig. 6 The colliding process of two planar and nonplanar IASWs of compressive colliding process geometry at the same values as in fig.2

        After the interaction, one can note that the trajectories of the rarefactive and compressive IASWs have deviated from the initial trajectories. In fact, these deviations are just the phase shifts for two IASWs [33]. Physically, this means that the negative ion-to-positive ion density ratio has an important effect on the dynamical behavior (i.e., rarefactive or compressive) of IASWs. This agrees with result obtained by El-Labany et al. [43].

IV. SOLITONS AND PHASE SHIFTS AT CRITICAL NEGATIVE IONS DENISTY:

        In this section we take the ion densities to be critical μ_{2c}, with $A = 0$. Without loss of generality, the quadratic nonlinearity in the KdV equations 13-14 disappears, and $\varphi_{2\xi} = 0$ and $\varphi_{2\eta} = 0$, but $\widehat{\varphi}_2 \neq 0$, and we must keep the contributions in the first order perturbation solutions. Accordingly, Eq. 10 becomes

$$n_{-}^{(2)} = \frac{3\beta^2}{2\lambda^4}\left(\varphi_{1\xi}^2 + \varphi_{1\eta}^2\right) \quad (27a) \qquad u_{+}^{(2)} = \frac{1}{2\lambda^3}\left(\varphi_{1\xi}^2 - \varphi_{1\eta}^2\right), \qquad (27c)$$

$$n_+^{(2)} = \frac{3}{2\lambda^4}\left(\varphi_{1\xi}^2 + \varphi_{1\eta}^2\right), \quad (27b) \qquad u_-^{(2)} = \frac{\beta^2}{2\lambda^3}\left(\varphi_{1\xi}^2 - \varphi_{1\eta}^2\right). \qquad (27d)$$

where $\delta_1 \neq 0$.

At critical negative ion density, the third order variables becomes

$$\lambda\widehat{T}n_+^{(3)} + \widehat{\widetilde{T}}n_+^{(1)} + \frac{\nu}{R}u_+^{(1)} \qquad\qquad \lambda\widehat{T}u_+^{(3)} + \widehat{R}\varphi_1 + \widehat{\widetilde{T}}u_+^{(1)}$$
$$+ \widehat{R}u_+^{(3)} \qquad (28a) \qquad\qquad + \widehat{R}\varphi_3 \qquad (28c)$$
$$+ \widehat{\widetilde{R}}u_+^{(1)} = 0, \qquad\qquad\qquad = 0,$$

$$\lambda\widehat{T}n_-^{(3)} + \widehat{\widetilde{T}}n_-^{(1)} + \frac{\nu}{R}u_-^{(1)} \qquad\qquad \lambda\widehat{T}u_-^{(3)} - \beta\widehat{\widetilde{R}}\varphi_1 + \widehat{\widetilde{T}}u_-^{(1)}$$
$$+ \widehat{R}u_-^{(3)} \qquad (28b) \qquad\qquad - \beta\widehat{R}\varphi_3 \qquad (28d)$$
$$+ \widehat{\widetilde{R}}u_-^{(1)} = 0, \qquad\qquad\qquad = 0.$$

$$\left(\frac{\partial^2}{\partial\xi^2} + 2\frac{\partial^2}{\partial\xi\partial\eta} + \frac{\partial^2}{\partial\eta^2}\right)\varphi_1 - \mu_1\frac{\kappa - \frac{1}{2}}{\chi}\varphi_3$$
$$- \mu_1\frac{\left(\kappa - \frac{1}{2}\right)\left(\kappa + \frac{1}{2}\right)(\kappa + \frac{1}{2})}{6\chi^3}\varphi_1^3 - \mu_2 n_-^{(3)} + n_+^{(3)} \qquad (28e)$$
$$= 0$$

Solving equations containing the terms depending on ξ or η, besides τ we obtain the modified cylindrical Korteweg-de Vries (mcKdV) equations.

$$\frac{\partial\varphi_{1\xi}}{\partial R} + C\varphi_{1\xi}^2\frac{\partial\varphi_{1\xi}}{\partial\xi} + B\frac{\partial^3\varphi_{1\xi}}{\partial\xi^3} + \frac{\nu}{2R}\varphi_{1\xi} = 0, \qquad (29a)$$

$$\frac{\partial\varphi_{1\eta}}{\partial R} + C\varphi_{1\eta}^2\frac{\partial\varphi_{1\eta}}{\partial\eta} + B\frac{\partial^3\varphi_{1\eta}}{\partial\eta^3} + \frac{\nu}{2R}\varphi_{1\eta} = 0. \qquad (29b)$$

$$\frac{\partial P_0}{\partial\eta} = -E\varphi_{1\eta}^2, \qquad\qquad (29c) \quad \frac{\partial Q_o}{\partial\xi} = -E\varphi_{1\xi}^2, \qquad\qquad (29d)$$

where $C = \frac{15(1+\mu_2\beta^3)}{4\lambda^4(1+\mu_2\beta)}$, and $E = \frac{(1+\mu_2\beta^3)}{8\lambda^4(1+\mu_2\beta)}$.

Because mKdV equations like 29a and 29b are invariant for a sign inversion of $\varphi_{1\xi}$ or $\varphi_{1\eta}$ the one-soliton solutions can be written as

$$\varphi_{1\xi} = \pm\varphi_{0\xi}\theta_1^\nu\text{sech}\left(\varphi_{0\xi}\sqrt{\frac{C}{6B}}\,\theta_1^\nu\left[\xi - \frac{1}{6}C\varphi_{0\xi}^2\theta_1^{2\nu}R\right]\right), \qquad (30)$$

$$\varphi_{1\eta} = \pm\varphi_{0\eta}\theta_2^\nu\text{sech}\left(\varphi_{0\eta}\sqrt{\frac{C}{6B}}\,\theta_2^\nu\left[\eta - \frac{1}{6}C\varphi_{0\eta}^2\theta_2^{2\nu}R\right]\right). \qquad (31)$$

where $\varphi_{0\xi}$ and $\varphi_{0\eta}$ are the maximum amplitudes of IASWs in their initial position. Note that the respective $\pm$ signs are not coupled. After the same

mathematical strategy that is used in Sec. III, we finally obtain the corresponding phase shifts after collision of the two IASWs in the critical case.

$$\Delta P_c = 2\varepsilon^2 E \varphi_{0\eta} \left(\frac{6B}{C}\right)^{1/2} \theta_2^\nu, \tag{32}$$

$$\Delta Q_c = -2\varepsilon^2 E \varphi_{0\xi} \left(\frac{6B}{C}\right)^{1/2} \theta_1^\nu. \tag{33}$$
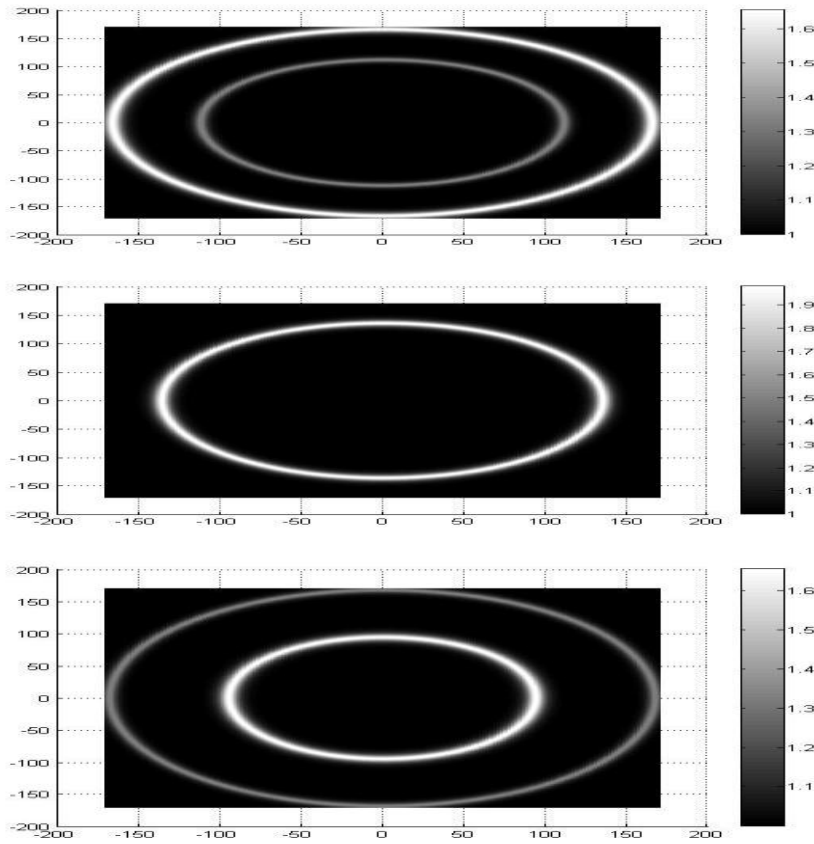

Fig. 7 In the critical case, the contour plot for the colliding process of two dark/bright IASWs at the planar case $\nu = 0$ at different times a)t = 0, b)t = 25 and c)t = 55.

V. CONCLUSIONS

Finally, we conclude the critical case, it is important to mention that the interaction of the IASWs in planar one-dimensional geometry, cylindrical, and spherical geometry are different
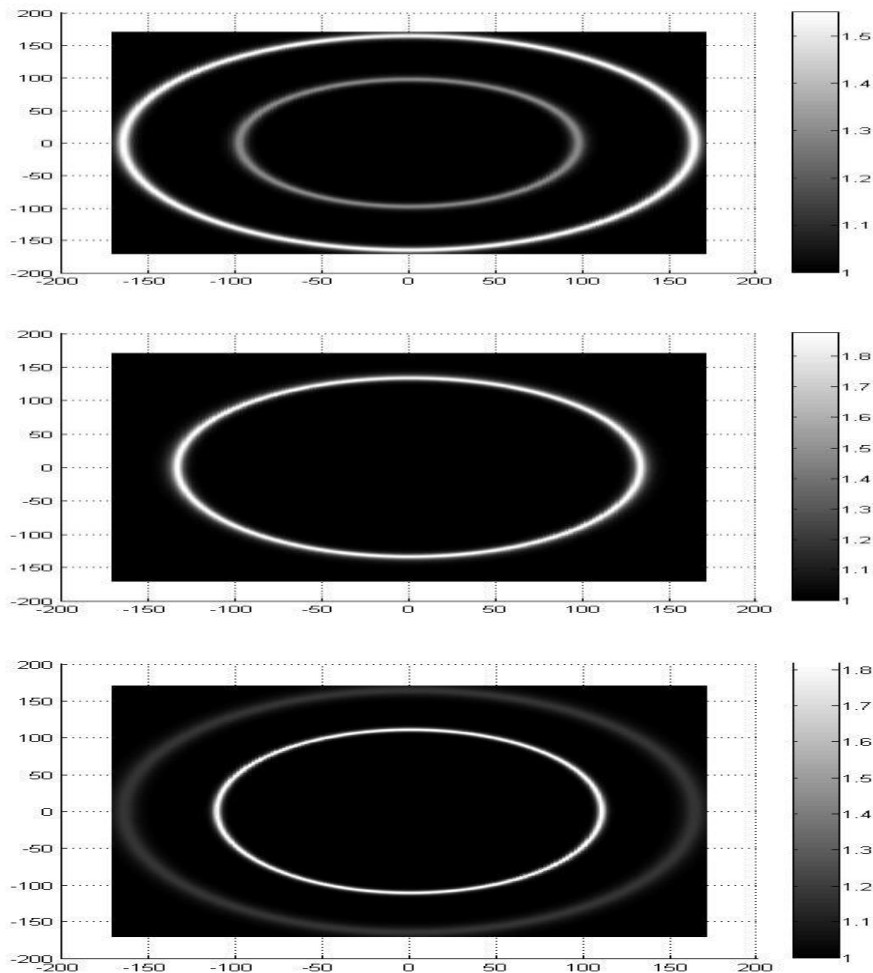
Fig. 8 In the critical case, the contour plot for the colliding process of two dark/bright IASWs at the cylindrical case $v = 1$ for the same values as in fig.10 at different times a)$t = 0$, b)$t = 42$ and c)$t = 75$.

Figures 7(a)-7(c) [8(a)-8(c) and 9(a)-9(c)] represents the contour plot for the colliding processes between two bright/dark planar [cylindrical and spherical] IASWs at different times which admits combination of bright and dark IASWs collision agrees with [43]. It's clear that the two bright/dark of planar and nonplanar IASWs interact to create single composite structure at different times. This behavior may explain as follows: the wave speed for planar IASWs is greater than the cylindrical and the spherical IASWs and cylindrical IASWs are much greater than spherical IASWs.
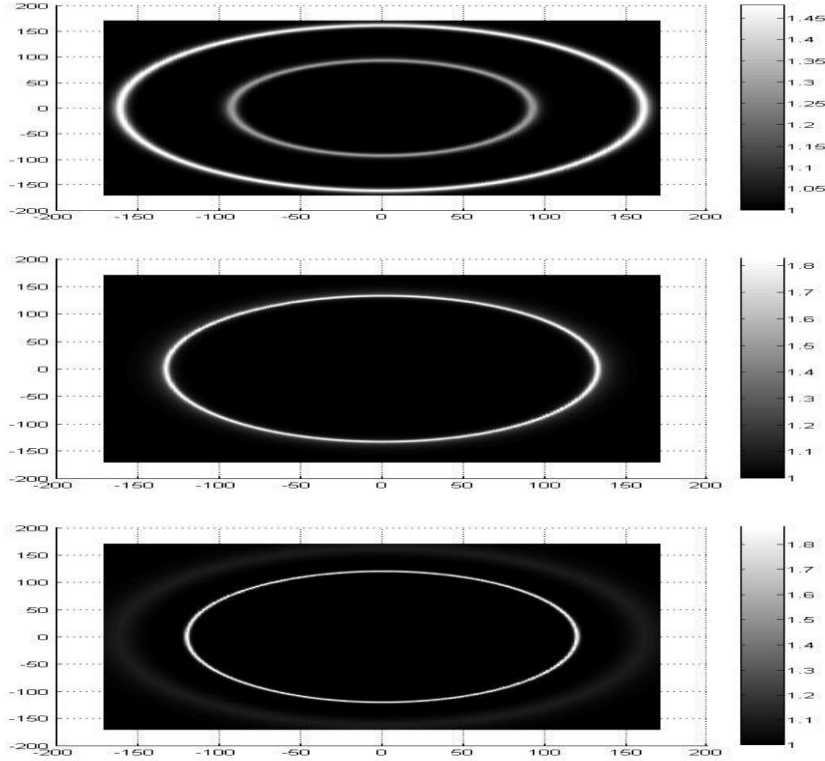
Fig. 9. In the critical case, two dark/bright IASWs at the spherical case ν = 2 for the same values as in fig.10 at different times a)t = 0, b)t =50 and c)t = 80.
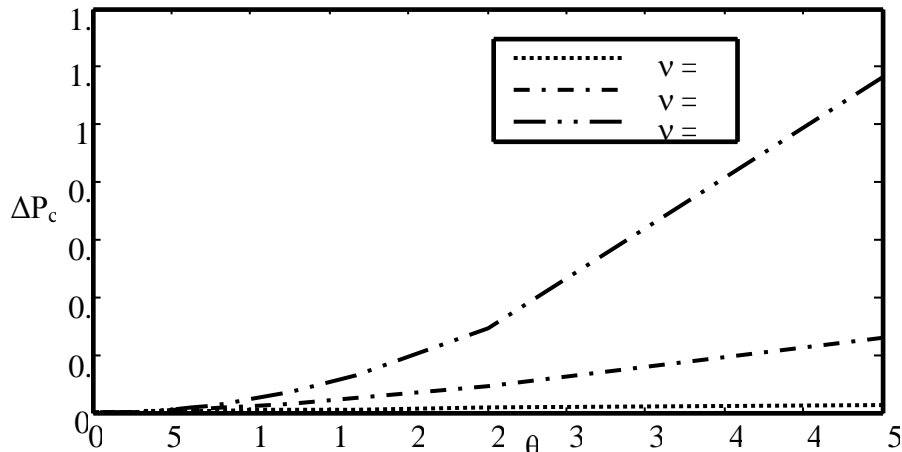

Fig. 10, The variation of the phase shift ΔPc with θ (ν = 0) for planar geometry, (ν = 1) for cylindrical geometry, and (ν = 2) for spherical geometry

Fig.10 explores the difference in phase shifts ΔP_c for planar and nonplanar geometries at the critical case. If the angle $\theta \leq 10$ the planar geometry approach the nonplanar geometries but when $\theta \geq 10$ they became to be far away from each other.
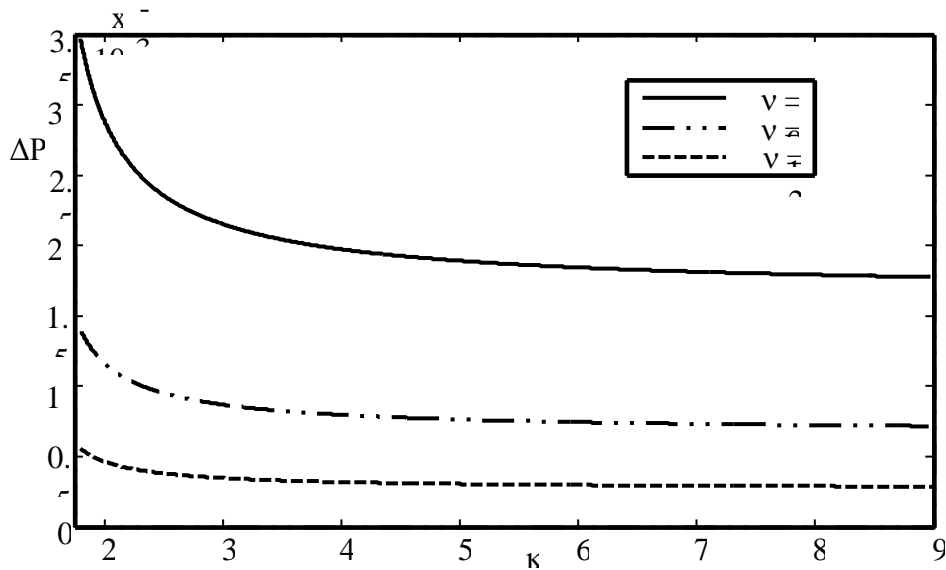

Fig. 11, The variation ΔPc with κ ($\nu = 0$) for planar geometry, ($\nu = 1$) for cylindrical geometry, and ($\nu = 2$) for spherical geometry

Fig. 11 represents the phase shifts change the superthermal parameter κ for planar and nonplanar (cylindrical, and spherical) geometry. For a given value of ν, the phase shift curves decreases rabidly until $\kappa=5$ for the planar geometry and almost $\kappa=3$ for the cylindrical geometry and the spherical geometry. Figures 12 show the variations of the negative ion-to-positive ion density ratio against the space coordinate x and the time variable t, respectively, for the critical case.

Continuously, Figs 12 ensure that the compressive IASWs propagate in opposite directions approach to each other, collide, and asymptotically separate away, respectively. After the interaction, one can note that the trajectories of compressive IASWs have deviated from the initial trajectories for the planar and the nonplanar geometry. This agrees with result obtained [43]
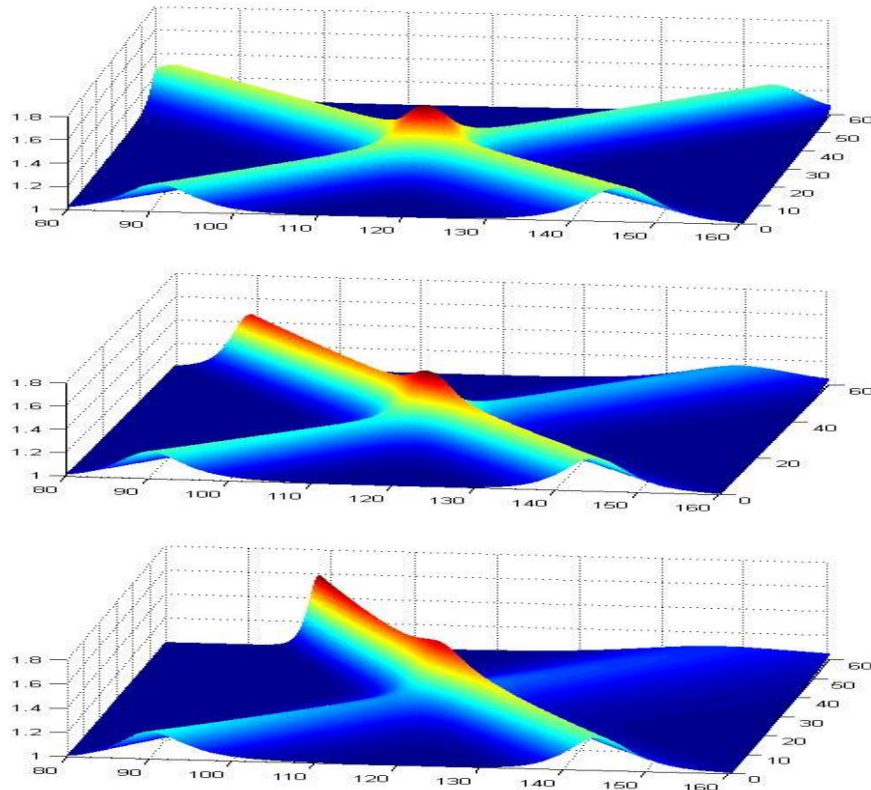
Fig. 12 The colliding process of two planar and nonplanar IASWs of compressive colliding process geometry at the same values as in fig.7

In this manuscript we considered a multicomponent plasma consisting of mobile positive and negative ions, and superthermal electrons in planar and nonplanar geometry. Accordingly, we employed the extended PLK method, the nonlinear mcKdV equations and their change in trajectories were derived. For the generic case, the nonlinear propagation and the collision of IASWs are described by nonlinear cKdV equations and their corresponding phase shifts. Furthermore, the effects of some plasma parameters such as; the negative ion-to-positive ion density ratio μ_2, superthermal parameter κ, and the positions of IASWs r on dynamics and collisions of IASWs are discussed and graphically displayed. In particular, it is found that negative ion-to-positive ion density ratio play an important role in the planar and nonplanar geometry not only on the formations and the dynamical behavior of IASWs, but also on the IASWs collision which translated in the presented phase shifts.

REFERENCES

[1] Bharuthram R.; and P. K. Shukla (1986). Large amplitude ion acoustic double layers in a double Maxwellian electron plasma Phys. Fluids 20: 3214.

[2] Yadav L. L.; and S. R. Sharma (1991). Obliquely propagating ion-acoustic double layers in a multicomponent magnetized plasma Phys. Scr. 43: 106

[3] Agrimson E.; N. D'Angelo; and R. L. Merlino; (2001). Excitation of ion-acoustic-like waves by subcritical currents in a plasma having equal electron and ion temperatures. Phys. Rev. Lett. 86: 5282

[4] Sabry R.; W. M. Moslem; and P. K. Shukla (2009). Fully nonlinear ion-acoustic solitary waves in a plasma with positive-negative ions and nonthermal electrons Phys. Plasmas 16: 032302

[5] Ikezi H.; R. Taylor; and D. Baker (1970). Formation and Interaction of Ion-Acoustic Solitions Phys. Rev. Lett. 25: 11

[6] Tran M.Q. (1979). Ion Acoustic Solitons in a Plasma: A Review of their Experimental Properties and Related Theories Phys. Scr. 20: 317

[7] Nakamura Y. (1982). Ion acoustic shock waves in weakly relativistic and dissipativeplasmas with nonthermal electrons and thermal positrons IEEE Trans. Plasma Sci. PS-7: 232

[8] Lonngren K.E. (1983). Ion acoustic shock waves in weakly relativistic and dissipative plasmas with nonthermal electrons and thermal positrons Plasma Phys. 25: 943

[9] Infeld E.; and G. Rowlands; (1992). Nonlinear Waves, Solitons and Chaos (Cambridge Univ. Pres, Cambridge)

[10] Washimi H.; and T. Taniuti; (1966). Propagation of Ion-Acoustic Solitary Waves of Small Amplitude Phys. Rev. Lett.17:996

[11] Maxon S.; and J. Viecelli (1974). Cylindrical solitons Phys. Fluids 17: 1614

[12] Hershkowitz N.; and T. Romesser; (1974). Observations of Ion-Acoustic Cylindrical Solitons Phys. Rev. Lett. 32: 581

[13] Ko K.; and H. H. Kuehl; (1979). Cylindrical and spherical Korteweg–deVries solitary waves Phys. Fluids 22:1343

[14] Nakamura Y.; M. Ooyama; and T. Ogino; (1980). Interaction of the non-planar dust ion-acoustic solitary waves Phys. Rev. Lett. 45: 1965

[15] Eslami P.; M. Mottaghizadeh; and H. R. Pakzad; (2011). Effect of ion temperature on ion-acoustic solitary waves in a plasma with a q-nonextensive electron velocity distribution. Phy. of Plasmas 18(7)

[16] Podesta J.J.; (2005). Spatial Landau damping in plasmas with three-dimensional κ distributions Phys. Plasmas 12: 052101

[17] Baluku T. K., and M. A. Hellberg; (2008). Comment on "Mathematical and physical aspects of Kappa velocity distribution Phys. Plasmas 15: 123705

[18] Sultana S.; I. Kourakis; N.S. Saini; M. A. Hellberg (2010). Oblique electrostatic excitations in a magnetized plasma in the presence of excess superthermal electrons. Phys. Plasmas 17: 032310

[19] El-Awady E. L.; S. A. El-Tantawy; W. M. Moslem; and P. K. Shukla; (2010). Electron–positron–ion plasma with kappa distribution: Ion acoustic soliton propagation. Phys. Lett. A 374: 3216

[20] Ghosh D. K., P. Chatterjee, and B. Sahu (2012). Superthermal effect of electrons on nonplanar dust-ion-acoustic solitary waves and double layers in a dusty plasma.Astrophysics and Space Science; 342

[21] Huang G. X.; and M. G. Velarde; (1996). Head-on collision of two concentric cylindrical ion acoustic solitary waves Phys. Rev. E 53: 2988

[22] Han J. N.; S. C. Li; X. X. Yang; and W. S. Duan; (2008). Head-on collision of ion-acoustic solitary waves in an unmagnetized electron-positron-ion plasma Eur. Phys. J. D 47:197.

[23] Chatterjee P.; U. Ghosh; K. Roy; S. V. Muniandy; and C. S. Wong; (2010). Head-on collision of ion acoustic solitary waves in an electron-positron-ion plasma with superthermal electrons Phys. of Plasmas 17: 122314

[24] Shahmansouri M.;and M. Tribeche; (2014). Ion acoustic solitary waves in bi-ion plasma with superthermal electrons Astrophys Space Sci. 349

[25] Ning Han J.; J. Xiu Li; J. Hua Luo; G. Hua Sun; Z. Lai Liu; S. Hong Ge; and X. Xing Wang; (2014). Physics of Plasmas ;89.

[26] Gardner C. S.; J. M. Greener; M. D. Kruskal; and R. M. Miura; (1967). Method for solving the Korteweg-deVries equation Phys. Rev. Lett. 19: 1095

[27] **Su C. H.; and R. M. Mirie; (1980).** Head-on collision of ion acoustic solitary waves in an electron-positron-ion plasma with superthermal electrons. J. Plasma Phys. 98: 509

[28] **Xue J. K.; (2006).** Interaction of solitary waves in magnetized warm dusty plasmas with dust charging effects. Chin. Phys.15: 562

[29] **Han J. N.; X. X. Yang; D. X. Tian; and W. S. Duan; (2008).** Head-on collision of ion-acoustic solitary waves in a weakly relativistic electron–positron–ion plasma Phys. Lett. A, 372: 4817

[30] **El-Shamy E. F.; W. M. Moslem; and P. K. Shukla; (2009).** Head-on collision of ion-acoustic solitary waves in a weakly relativistic electron–positron–ion plasma Phys. Lett. A, 374: 290

[31] **EL-Shamy E. F.; (2009).** Head-on collision of ion thermal waves in a magnetized pair-ion plasma containing charged dust impurities Phys. Plasmas 16: 113704

[32] **Liang G. Z.; J. N. Han; M. M. Lin; J. N. Wei; and W. S. Duana; (2009).** Collisional phase shifts between two colliding solitary waves in a three-dimensional magnetized dusty plasma. Phys. Plasmas 16: 073705

[33] **Verheest F.; M. A. Hellberg; and W. A. Hereman; (2012).** Head-on collisions of electrostatic solitons in multi-ion plasmas Phys. Plasmas 19: 092302

[34] **Verheest F.; M. A. Hellberg; and T. K. Baluku; (2012).** Arbitrary amplitude ion-acoustic soliton coexistence and polarity in a plasma with two ion species Phys. Plasmas 19: 032305

[35] **Ghorui M. K.; U. K. Samanta; and P. Chatterjee; (2013).** Head-on collisions of ion-acoustic Korteweg-de Vries/modified Korteweg-de Vries solitons in a magnetized quantum electron-positron-ion plasma Ap&SS, 345: 273

[36] **Mehdipoor M.; (2012).** High-precision analysis of the solar twin HIP 100963 Ap&SS, 348: 115

[37] **El-Shamy E. F.; (2014).** Multi-dimensional instability of obliquely propagating ion acoustic solitary waves in electron-positron-ion superthermal magnetoplasmas Phys. Plasmas 21: 082110

[38] **EL-Labany S. K.; E. F. EL-Shamy; and M. G. El-Mahgoub; (2012).** The interaction between two planar and nonplanar quantum electron acoustic solitary waves in dense electron-ion plasmas Phys. Plasmas 19: 062105

[39] El-Labany S. K.; E. F. EL-Shamy; and M. Abu El-Eneen; (2012). The interaction between two planar and nonplanar quantum electron acoustic solitary waves in dense electron-ion plasmas. Ap&SS, 337:275,

[40] Fraunie P.; and Y. Stepanyants; (2002). Decay of cylindrical and spherical solitons in rotating media Phys. Lett. A, 293: 166

[41] El-Shamy E. F.; F. S. Gohman; (2014). Propagation and collision of soliton rings in quantum semiconductor plasmas.Phys. Lett. A, 378: 2688

[42] Li S. C.; (2010). The effects of Bohm potential on ion-acoustic solitary waves interaction in a nonplanar quantum plasma Phys. Plasmas 17: 082307

[43] El-Labany S. K.; E. F. El-Shamy; N. A. El-Bedwehy; and M. Shokry; (2016). Head-on-collision of modulated dust acoustic waves in strongly coupled dusty plasma Phys. Plasmas 23

التصادم للموجات السولوتينية المضيئة والمظلمة في بلازما عديدة المكونات بها الكترونات فوق حراريه في احداثيات مختلفة

محمد شكري

قسم الفيزياء – كلية العلوم –جامعة دمياط

تم دراسة التصادم الخطي والغير خطي للموجات السلوتونية الغبارية في بلازما تحتوي علي نوعان من الايونات الموجبة والسالبة وتوزيع قابا للالكترونات الفوق حرارية . وجد ان في الحالة العامة بواسطة استخدام طريقة PLK هناك نوعان من المعادلة KdV وتم دراسة ازاحة الطور للموجات المضيئة والمظلمة.

في الحاله الخاصة عندط تركيز معين للايونات تم استخدام طريقة PLK واستنتاج المعادلة المعدله ل KdV لازاحة الطور الخاصه بها قد وجد ان نوعان من الموجات الخطية والغير خطية المضيئة والمظلمة علي الترتيب يمكنهم الانتشار والاصطدام ببعضهما في كلا الحالات. تم دراسة تاثير بعض المتغيرات مثل النسبة بين تركيز الايونات السالبة الي الموجبة – معامل الفوق حراري للالكترونلت علي التصادم

النتائج الرياضية لهذا البحث تتنبا بخصائص التصادم للموجات السولونينية الغبارية في المعمل وتفاعلات البلازما